Analysis of Road-User Interaction by Extraction of Driver Behavior Features Using Deep Learning

Arianna Bichicchi, Rachid Belaroussi, Andrea Simone, Valeria Vignali, Claudio Lantieri, Xuanpeng Li

IEEE Access
Multidisciplinary | Rapid Review | Open Access Journal

Received October 30, 2019, accepted December 19, 2019, date of publication January 13, 2020, date of current version January 30, 2020.

Digital Object Identifier 10.1109/ACCESS.2020.2965940

Analysis of Road-User Interaction by Extraction of Driver Behavior Features Using Deep Learning

ARIANNA BICHICCHI[1], RACHID BELAROUSSI[2], ANDREA SIMONE[1], VALERIA VIGNALI[1], CLAUDIO LANTIERI[1], AND XUANPENG LI[3]

[1]Department of Civil, Chemical, Environmental and Materials Engineering, School of Engineering and Architecture, University of Bologna, 40136 Bologna, Italy
[2]COSYS-GRETTIA, French Institute of Science and Technology for Transport, Development and Networks, Gustave Eiffel University, 77447 Marne-la-Vallée, France
[3]School of Instrument Science and Engineering, Southeast University, Nanjing 210096, China

Correspondin g author: Arianna Bichicchi (arianna.bichicchi2@unibo.it)

ABSTRACT In this study, an improved deep learning model is proposed to explore the complex interactions between the road environment and driver's behaviour throughout the generation of a graphical representation. The proposed model consists of an unsupervised Denoising Stacked Autoencoder (SDAE) able to provide output layers in RGB colors. The dataset comes from an experimental driving test where kinematic measures were tracked with an in-vehicle GPS device. The graphical outcomes reveal the method ability to efficiently detect patterns of simple driving behaviors, as well as the road environment complexity and some events encountered along the path.

INDEX TERMS Deep learning, driver behavior, event detection, road safety, workload.

I. INTRODUCTION

Road safety is today one of the most actual and challenging field of research, as road fatalities continue to increase year after year with dramatic social and economic impacts [1]. Because of the factors associated to fatal road accidents, most studies are addressed to human factors who aspire to analyze the driver behaviour. The entire process of observation, modelling, visualization and prediction of driving behaviour unavoidably presuppose the development of experimental tests who produce large amount of data. Both simulated and semi- or naturalistic tests are provided with different types of sensors aiming to record all possible information from the driver and from the vehicle, together with their interactions.

As deep learning methods may help in the processing of high-dimensional data, their application in transportation field has been increasing recently. Applications are mainly related to traffic flow forecasting, crashes prediction and driver behaviour analyses.

Studies focusing on driver behavior analysis presuppose that the design and selection of the features is based on researchers experience and finding an appropriate method for their representation is often difficult, especially for driving behaviors that are obtained from a driver–vehicle–environment system [2].

Most of the studies aiming to extract latent features from multi-dimensional time-series data were performed by using the Principal Component Analysis. PCA is used to decompose a multivariate dataset in a set of successive orthogonal components that explain a maximum amount of the variance [3]. Despite the several conducted studies, it is difficult to adopt PCA for extracting time series of latent features from driving behaviour data because vehicle dynamics and the driver behaviour have non-linear properties, whereas PCA is based on linear transformations. This problem can be solved by using Kernel Principal Component Analysis (KPCA), because it uses a non-linear kernel function that involves a non-linear transformation for mapping the data to a high-dimensional space. Then, KPCA employs PCA to extract latent features in the high-dimensional space. Indeed, Zhao successfully extracted latent features for driver mental fatigue classification using KPCA, proving that this method is more accurate than PCA [4]. Nevertheless, when a large amount of driving behaviour data is used for analysis, the computational cost of KPCA is high because the kernel method has to compute a matrix in $RN \times N$, where N is the total number of frames of data.

Dong made the first attempt by adopting a deep neural architecture, based on Convolutional Neural Network (CNN)

The associate editor coordinating the review of this manuscript and approving it for publication was Haiyong Zheng.

and Recurrent Neural Network (RNN), for the first time in order to extract features directly from GPS. This because those neural networks can learn high level driving style features from the low level feature matrices requiring less human work than the previous methods, that rely on handcrafted driving behaviour features [5].

A particular case of driver behaviour analysis is the one by Dwivedi who proposed a vision based on CNN to detect driver drowsiness. According to this, the caption of various latent facial features and complex non-linear feature interactions were possible [6].

Other studies have proved that an algorithm based on the Back Propagation (BP) provides good results because it can approximate any non-linear continuous function with arbitrary precision. Meseguer used this kind of neural network to dynamically and automatically analyze users data in order to identify the driving style as well as the category of road segment profile [7]. This type of neural network results are effective not only for vehicle dynamics and geographic data, but also for training and testing features in order to improve the road type recognition rate based on images [8].

The development of several applications including tasks based on unsupervised methods for driver behaviour detection have started only a few years ago [9]. In case of large dataset generated by non-linear transformations, unsupervised learning methods are able to extract latent features of driving behavior without using label information. In particular, recent studies involved this method to enable reliable driving behaviour visualization output. The review of driving behaviour can be a key practice for the improvement of driving behaviour and safe driving promotion [10].

Considered the importance of using a denoising criterion as a tractable unsupervised objective to guide the learning of useful higher-level representations [11], in this study has been chosen to exploit a Denoising Stacked-Autoencoder (SDAE) to extract the latent features for a deep driving behavior analysis.

It is worth noting the importance of such research, which also aims at being able to provide real time information and consequently safety advices for the prevention of road crashes. Indeed, it is supposed that deep learning will be able to accurately predict driver behaviour patterns, attracting relevant attention for the potential role in autonomous driving applications.

II. METHODS

The objective of this study is to use SDAE for extracting the driving behaviour features from a dataset from a real driving test and recorded by an in-vehicle GPS sensor. Regarding data source, current research suggests that in-vehicle data (CAN-BUS) can be used as an effective representation of driving behaviour for recognizing different drivers [12]. Similarly, other studies involve GPS receiver [13] for simple data extraction and potential usability in large scale research.

The proposed method implements a deep sparse autoencoder (SDAE) to extract the lowdimensional high-level representation from high-dimensional raw driving behavioral dataset. According to the resulting low-dimensional representation, two visualization methods are suggested. The first is a cubic representation displaying extracted three-dimensional features. The second is a colored trajectory showing on the path driven the color expression of the extracted features. The color results from an RGB color space combination corresponding to the extracted three-dimensional features.

FIGURE 1. VBOX GPS/camera data logger.

A. EXPERIMENTAL SETUP

The data collection used the Racelogic Video V-Box Pro device (FIGURE 1), an in-car video system installed on the test vehicle. The reliability of this device for data analysis have been tested several road safety studies [14], [15]. The device combines a 10Hz GPS data logger with a two cameras video system, with an accuracy of 0.5 meters and 0.2 km/h. The output consisted in a .csv file with a data recording period of 0,1s. Every recording included information on positioning coordinates (latitude and longitude), time and several kinematic data. With reference to this study, the six typologies of kinematic data considered are:

- Longitudinal speed (km/h);
- Vertical speed (km/h);
- Longitudinal Acceleration (m/s^2);
- Transversal Acceleration (m/s^2);
- ComboG (combination of g forces);
- Heading of the vehicle (deg);

For the scope of this research, a real driving test has been conducted and driving behavior data of 10 participants have been collected.

The driving tests were run within the industrial zone of Casalecchio di Reno (Bologna – Italy) on a circuit route of 2500 meters. The first 1000 meters, red in FIGURE 2 consisted of a complex road stretch with many entrances and traffic while the last 1500 meters, blue in FIGURE 2, until the starting point consisted of a road stretch with a simpler driving complexity [16], [17].

All participants were asked to drive for two testing sessions (approximatively one in the morning and one in the afternoon). As summarized in TABLE 1, each driving session included three laps of the circuit route: the first dedicated to the user' adaptation to the experimental conditions, the second to test the driving performance without any external event occurring (''baseline lap'') and the third to test the driving

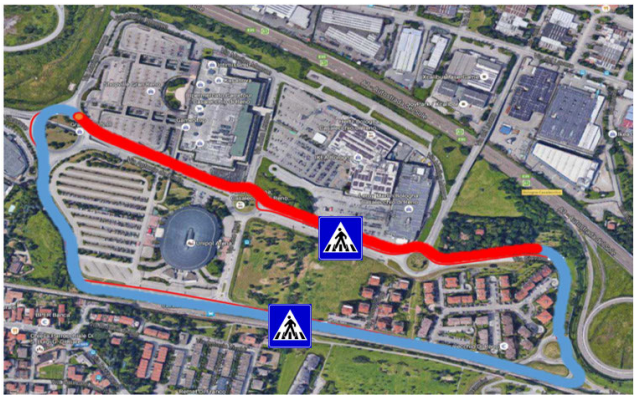

FIGURE 2. Driving route.

TABLE 1. Driving test features and variables.

LAP SCHEDULE	
Lap 0	Adaptation to the experimental settings (dataset not used)
Lap 1	Baseline
Lap 2	Test with external events (2 pedestrians crossing the road on crosswalks)
ROAD COMPLEXITY	
Complex (red color)	Road section with three lanes for direction, many entrances and traffic jams, commercial area
Easy (blue color)	Road section with one lane for direction, residential area

performance in reaction to two workload inducing simulated events (''test lap'') consisting of a pedestrian crossing the road on a crosswalk (one on the ''complex'' segment and the other on the ''easy'' segment''). At the end of each driving session, participants were asked to subjectively evaluate their mental load (workload) while accomplishing the driving task throughout the standardized NASA-TLX survey.

One dataset sheet was elaborated for each test participant, accordingly to the scheduled data processing activities.

B. MODEL AND HYPERPARAMETERS TUNING

The developed DSAE model is able to extract time series of latent features through an encoding process, one for each hidden layer, minimizing the error computed with the cost function between the input time-series data and the decoded time-series data. According to the visualization method here proposed, the extracted features are drawn on a roadmap representing a colored trajectory.

In the following subparagraphs the developed model is described together with hyperparameters tuning activity. The goal of hyperparameters tuning is to select hyperparameters that will give good generalization performance. Typically, this works by estimating the generalization performance for different choices of hyperparameters (e.g. using a validation set), and then choosing the best.

Théano library was employed for model development of this study.

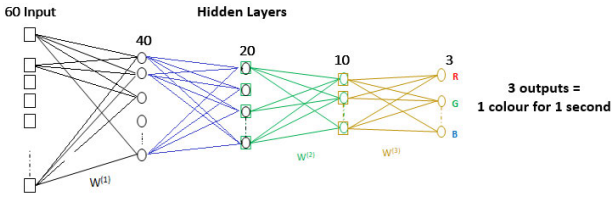

FIGURE 3. Architecture of the SDAE.

a: ACTIVATION FUNCTION

The chosen activation function consists in a hyperbolic tangent function f $(\cdot) = \tanh(\cdot)$ as has been evaluated that outperforms the traditional sigmoid function.

b: ARCHITECTURE

The chosen architecture consisted in the scheme in FIGURE 3:

- Input: 6 data inputs x 10 data measurements over 1s = 60 inputs for a sliding window.
- Encoding hidden layers (40, 20, 10);
- Output layer: 3 RGB colors. The RGB color space is ideal to represent driving behaviors, being a three-dimensional space. As the range of the RGB color space is [0, 1], the three-dimensional hidden features have been normalized into [0, 1]. In summary, the three-dimensional hidden features could be mapped to the RGB space by:

$$rgb_{t,d} = \frac{h_{t,d}^{(final)} - h_{min_d}^{(final)}}{h_{max_d}^{(final)} - h_{min_d}^{(final)}} \quad (1)$$

where:

- $rgb_{t,d}$ is a d-th element of a three-dimensional vector in the RGB space that represents the driving behaviour at the t-th time step.
- $\boldsymbol{h}_{t,d}^{(final)}$ is the d-th element of the extracted three-dimensional hidden feature's vector at the t-th time step;
- $\boldsymbol{h}_{\max,d}^{(final)}$ and $\boldsymbol{h}_{\min,d}^{(final)}$ are the minimum and maximum values of the d-th dimension in $\boldsymbol{h}(final)$, respectively.

c: NORMALIZATION

The measured driving behavior input data are defined as Y $\in$ RDY$\times$NY, where DY is the dimensionality and NY is the quantity of data (frames) in Y. Each dimension of Y represents one type of feature time-series data. The t-th frame of Y is defined as:

$$\boldsymbol{y_t} = (y_{t,1}, y_{t,2}, \ldots, y_{t,DY})^T \in \mathrm{R}DY \quad (2)$$

Considering the use of a hyperbolic tangent as activation function, the output range of the normalization process results is [-1,1].

To reconstruct the input data using the tanh function, each dimension of Y is independently normalized into [-1,1] by using the maximum and minimum values. Thus, the t-th

frame of the normalized data is expressed as:

$$\boldsymbol{x_t} = (x_{t,1}, x_{t,2}, \ldots, x_{t,DY})^T \in \mathrm{R}DY \tag{3}$$

where it is normalized by:

$$x_{t,d} = 2\left(\frac{y_{t,d} - y_{d_{min}}}{y_{d_{max}} - y_{d_{min}}}\right) - 1 \tag{4}$$

$$y_{d_{max}} = \max\left(y_{1,d}, \ldots, y_{NY,d}\right) \tag{5}$$

$$y_{d_{min}} = \min\left(y_{1,d}, \ldots, y_{NY,d}\right) \tag{6}$$

where y_{dmax} and y_{dmin} are the maximum and minimum values of the d-th dimension of Y, respectively.

d: WINDOWING

In the windowing process, the normalized data are aggregated with a slide window that converts the data of w frames into a vector.

Thus, the windowing time-series data in the t-th frame are expressed as:

$$\boldsymbol{h_t^{(1)}} = \left(\boldsymbol{x_{t-w+1}^T}, \boldsymbol{x_{t-w+2}^T}, \ldots, \boldsymbol{x_{DV}^T}\right)\boldsymbol{T} \in \boldsymbol{R}^{D\mathbf{H}} \tag{7}$$

and $\boldsymbol{DH} = w \times \boldsymbol{DY}$, $t \geq w$.

Finally, the obtained windowing time-series data are:

$$\boldsymbol{H^{(1)}} = \left\{\boldsymbol{h}_1^{(i)}, \boldsymbol{h}_2^{(i)}, \ldots, \boldsymbol{h}_{NH}^{(i)}\right\} \in \mathrm{R}^{D\mathrm{H}xN\mathrm{H}} \tag{8}$$

when the slide window moves along the time axis frame by frame.

Hence, $N\mathrm{H} = N\mathrm{Y}$-$w$+*1* frames of windowing time-series data are obtained.

e: REGULARIZATION AND GENERATION OF A DRIVING COLOR MAP

Since loss functions are a key part of any machine learning model, we define an objective against which the performance of the model is measured. The set of weight parameters learned by the model is determined by minimizing a chosen loss function. In this research, the chosen cost function to train layer (l) is the following:

$$O^{(l)}(\Sigma) = \frac{1}{2N_V}\sum_{t=1}^{N_V}\left\|\mathbf{W}_t^{l(T)}\mathbf{h}_t^{(l)} - \mathbf{h}_t^{(l)}\right\|^2 + \frac{\alpha}{2}\sum_{l=1}^{L-1}\left\|\mathbf{W}^{(l)}\right\|_2^2 + \beta\sum_{i=1}^{D_H^{(l)}}\mathrm{KL}(\omega||\bar{h}_i^{(m)}) \tag{9}$$

where:

- L is the number of layers;
- $\mathbf{h}_i^{(l)}$ is the activity of hidden layer (l);
- $\sum = \{\mathbf{W}\ (1), \cdots, \mathbf{W}\ (L\text{-}1), \mathbf{b}\ (1), \cdots, \mathbf{b}\ (L\text{-}1)\ \}$ and the three terms represent respectively the Reconstruction Error Term and two Regularization Terms;
- the second term is used as a penalty to prevent overfitting, limiting the elements of all the weights W(l) by the L2 norm. In addition, the parameter α controls the strength of the penalty term.

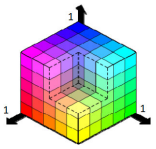

FIGURE 4. RGB Color Space.

- the third term is a sparse term ensuring data sparsity in the m-th layer and allows more obvious features to be obtained. The sparse term includes Kullback–Leibler divergence between two Bernoulli random variables with ω and $\mathrm{h}_\mathrm{i}^{(\mathrm{m})}$, where:

$$KL\left(\omega \parallel \bar{h}_i^{(m)}\right) = \omega\log\frac{\omega}{\bar{h}_i^{(m)}} + (1-\omega)\log\frac{1-\omega}{1-\bar{h}_i^{(m)}} \tag{10}$$

With ω as the sparsity target of the median layer and $\mathbf{h}$ *(t,i m)* as the i-th element of $\mathbf{h}(tm)$. Further, β controls the strength of the sparse term and when the sparse term is minimized, $\mathbf{h}_i^{(m)}$ is close to ω.

$$\bar{\boldsymbol{h}}_i^{(m)} = \frac{1}{2}\left(1 + \frac{1}{N_V}\sum_{t=1}^{N_V} h_{t,i}^{(m)}\right) \tag{11}$$

To generate a driving color map with different colors, an average value of the hidden features has been supposed as located in the center of the RGB color space. Therefore, a value of 0.5 has been set for ω because the center of each axis of the RGB color space is 0.5 (FIGURE 4). Thus, in the visualization method–driving color map, the generated colors do not tend to appear biased (e.g. reddish, bluish, etc.).

In order to monitor the Kullback–Leibler divergence, the plots reported in FIGURE 5 show the latent features moving towards the center of the RGB space, preserving information while ω increases). Since the range of the tanh function is [-1,1], the latent features result closer to 0, namely the center of the space.

Similarly, the same latent features can be plotted as time-series. In this case, the three extracted latent features are represented as time-series of three variables, namely the Red, Green and Blue color (FIGURE 6).

Therefore, in training the proposed model a backpropagation (BP) is implemented to raise reconstruction accuracy and, in the meantime, reduce the overfitting problem. The BP method performs partial differentiations of the weight matrices and biases for the objective function through chain rule. Therefore, the weight matrix $\mathbf{W}(l)$ and the bias vector $\mathbf{b}(l)$ between the l-th and *(l+1)*-th layers are updated by:

$$\mathbf{W}^{+(l)} \leftarrow \mathbf{W}^{(l)} - \eta^{(l)}\frac{\partial O(\sum)}{\partial \mathbf{W}^{(l)}}, \tag{12}$$

$$\mathbf{b}^{+(l)} \leftarrow \mathbf{b}^{(l)} - \eta^{(l)}\frac{\partial O(\sum)}{\partial \mathbf{b}^{(l)}}, \tag{13}$$

where $\mathbf{h}(l)$ represent the Learning Rate, equal for each hidden layer. To prevent the weight and bias from converging to an inaccurate local minimum, a greedy layer-wise training method is used.

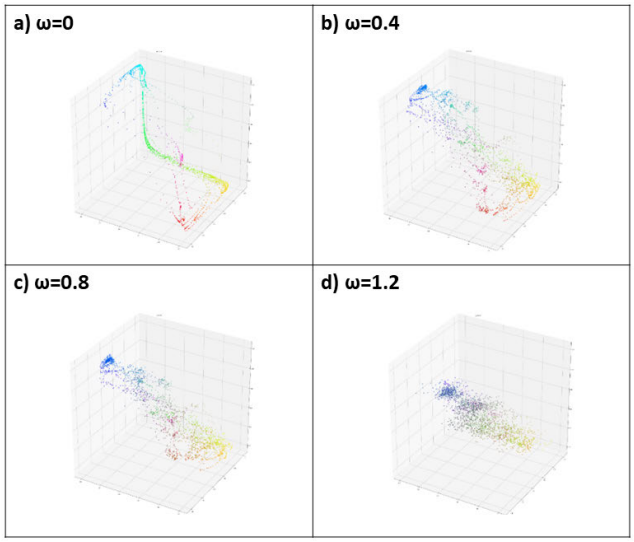

FIGURE 5. Latent features visualization with different ω values.

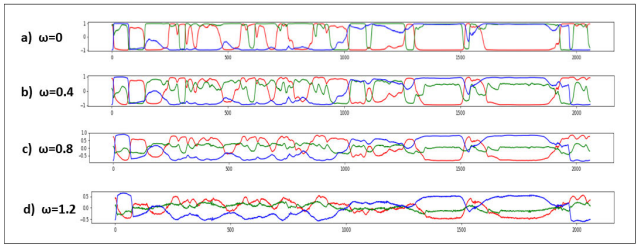

FIGURE 6. Latent features time-series with different ω values.

f: TRAINING AND VALIDATION

After the setting of all the necessary hyper-parameters, training and validation have been done on representative datasets. To evaluate the effectiveness of low-dimensional representation, the SDAE has been compared to other conventional methods from the viewpoint of linear separability of elemental driving behaviour. As a result, our methods outperformed other conventional methods in processing large amount of data.

The driving color maps generated by PCA, kernel PCA and DSAE for the 2nd and 3rd lap are shown in the FIGURE 7. Also, the observation of the extracted colors allowed the association with different selected "basic" driving behaviors, summarized in Table 2.

It is noticeable that other methods do not permit a differentiation of the same basic driving behaviors, as the generated colors are similar. For instance, more than one driving behavior (high speed forward and change in acceleration) correspond to a similar color (■) using the PCA. Similarly, the kernel PCA method characterized many driving behaviors with the same color (■) with slightly different shades.

Looking at the maps created with the PCA and kernel PCA it is possible to notice same segments with different colors. Obviously, this may be due to the driver behavior itself or just to a different combination of the input, but theoretically should not lead to different colors.

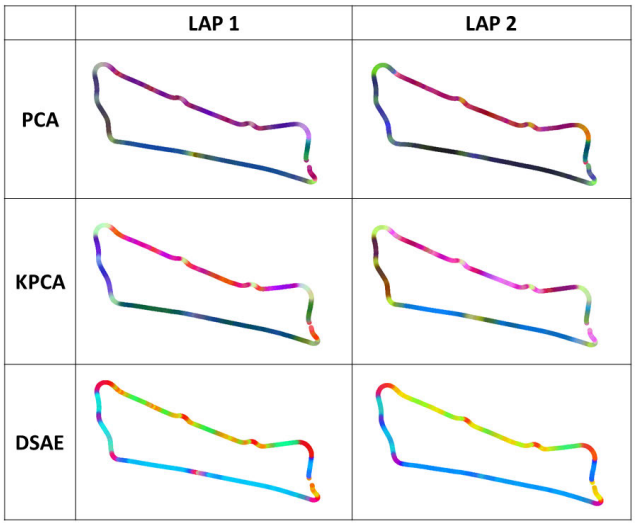

FIGURE 7. Model validation with driving color maps.

TABLE 2. Basic driving behaviors with representative colours.

	PCA	Kernel PCA	SDAE
High speed forward	■	■	■
Low speed forward	■	■	■
Accelerate / Decelerate	■	■	■
Turning left / right	■	■	■
Stopping vehicle	■	■	■

The latent features of the different methods (Table 2), as a last confimation, allow to discourage the use of PCA and kernel PCA for non-linear dataset as driving behaviour. Vice versa, the latent features extracted with DSAE look like roughly placed with the same criterion for each lap and, moreover, may allow to distinguish the different driver behaviors by their relative position in the latent space. That kind of result is mainly due to the regularization techniques applied to the neural network, that allow the DSAE to connect and arrange the features in the same way despite the different origin of the input feature.

III. DISCUSSION

The consequent testing of the model is discussed, as the main scope of this research is the identification of the previously mentioned experimental variables (TABLE 1) on the generated driving color maps. Testing has been done exploiting all the datasets from driving tests.

Trials were performed on datasheets containing one single lap of a driver. At a first glance, the chosen model resulted able to work any series of input data that concerns with the same features.

a: IDENTIFICATION OF ROAD COMPLEXITY

In order to verify the method capability to identify the type of road scenario (as previously anticipated in TABLE 1 and schematically reported in FIGURE 9, the route is composed

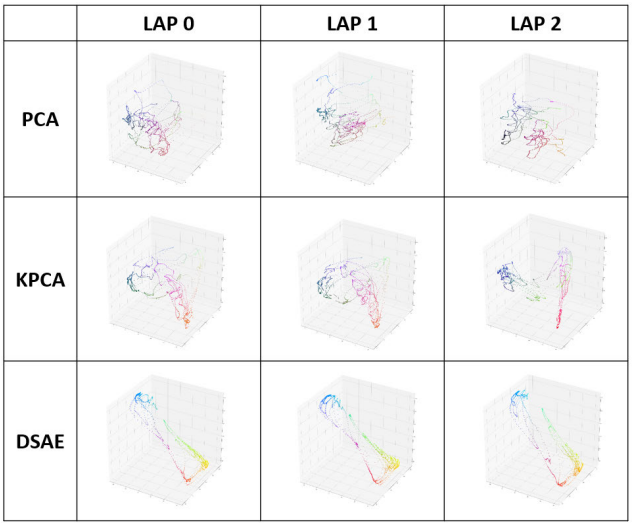

FIGURE 8. Model validation with features extraction in the latent space.

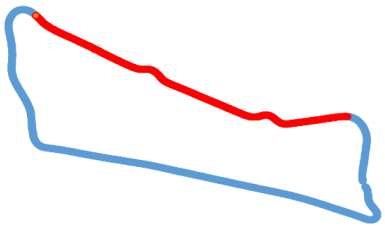

FIGURE 9. Complex (red) and easy (blue) driving situations.

by two segments defined as hard and simple context), have been tested the dataset of all drivers on the lap 3.

The complex contest refers the street Antonio de Curtis and have a complex road geometry (several lanes for both directions, intersections, roundabouts.). The simple contest refers instead to the streets Fausto Coppi and Giovannini that regards a residential area, with one lane for each direction of travel, low traffic volume.

The analysis of the obtained maps for all laps of all test participants (examples in FIGURE 10), fully confirms the identification of both contexts, as for all the maps the two road stretches have significantly different colors:

- The complex scenario - despite roundabouts and pedestrian crossings - results mainly in red or yellow/green color;
- The easy scenario results in blue colors.

b: DRIVER'S WORKLOAD

Subjective assessments have been proposed to measure driver effort during the driving task. The most common techniques are scales for the subjective mental workload. Examples are the NASA task load index, subjective workload assessment technique (SWAT) and the rating scale mental effort (RSME).

Among them, the NASA Task Load Index (NASA-TLX) is the most commonly used tool to rates the workload and most studies choose the standard NASA-TLX scales to conduct the subjective evaluations. More in detail, the tool includes

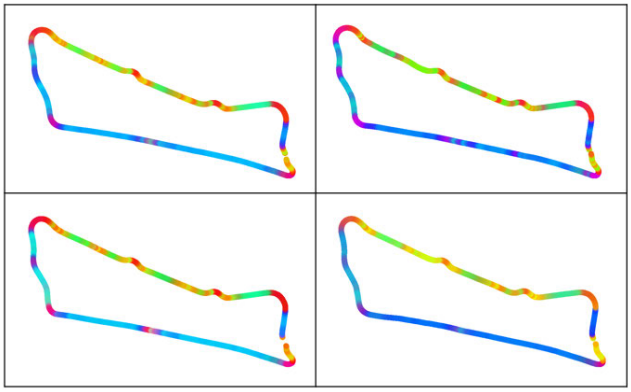

FIGURE 10. Example of Driving color maps for 4 drivers on Lap 3.

TABLE 3. NASA-TLX resulting scores.

Driver	TEST1	TEST2	Difference
1	39.0	24.3	-14.7
2	41.0	39.0	-2.0
3	28.0	23.3	-4.7
4	57.0	51.3	-5.7
5	31.7	24.7	-7.0
6	70.0	40.3	-29.7
7	34.7	20.3	-14.3
8	56.3	26.7	-29.7
9	53.0	38.3	-14.7
10	44.7	22.0	-22.7

a rating on six different subscales: Mental Demand, Physical Demand, Temporal Demand, Performance, Effort, and Frustration. They are rated for each task within a 100-points range with 5-point steps. The ratings are combined to the task load index by create an individual weighting of these subscales by letting the subjects compare them pairwise based on their perceived importance. This requires the user to choose which measurement is more relevant to workload. The number of times each is chosen is the weighted score. This is multiplied by the scale score for each dimension and then divided by 15 to get a workload score from 0 to 100, the overall task load index [18].

In this paper, the workload obtained with the NASA-TLX Test was compared to driving color map of each driver in order to evaluate if colors are predictive of the drivers' cognitive load.

The numerical results of NASA-TLX show a significant difference in workload between the two driving sessions for all the participants. In particular, the first test result is more demanding than the second, coherently with an increasing confidence with experimental conditions, and determining an average difference in workload score of -14.52 between all drivers (Table 3).

A comparison between the first and the second driving session for each driver was carried out. Indeed, any color difference resulted was attributable to a variation in workload.

The results obtained show that in the first test session the road path followed by the users is not particularly stressful from the point of view of mental load, considering that the evaluation range goes from 0 to 100 and the average workload of users is around 50 (with some exceptions such as user 6).

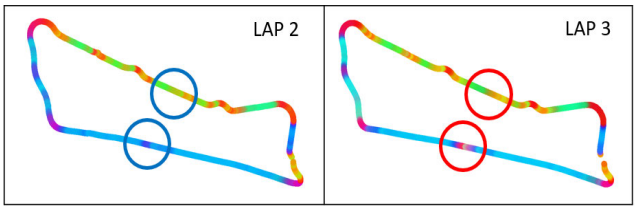

FIGURE 11. Pedestrians recognition between lap 2 and 3.

This indicates that drivers have been subject to an average level of strain. Comparing test 1 with test 2, we can see that, despite the increase in traffic during test 2, the value of the NASA-TLX score decreases for all users. This indicates that drivers tend to relax with respect to the initial test due to the previous knowledge of the track, the habitual effect of the track and the already known testing modes.

This trend is certainly caused by the habitual effect, i.e. the fact that in general a person who normally drives a road is subjected to a lower workload than a non-regular driver.

c: IDENTIFICATION OF EXTERNAL EVENTS

To verify the capability to graphically identify the presence of a pedestrian on the crosswalks, the 2nd and 3rd lap maps for each driver were compared with the expectation of a difference in the color pattern between the two maps (FIGURE 11). This difference results only for some drivers: color maps without pedestrian (lap 2) maps show orange color for the hard road context and dark blue color for the easy, while maps with pedestrian (lap 3) show dark orange shading into grey for the hard road context and reddish shades for the easy.

The overall precision of the method in recognizing pedestrians have been evaluated considering also false positive and negatives cases (True Positive = 13; False Positive = 4; False Negative = 3) and it resulted in a True Positive rate equal to 0,76 (TP/[TP+FP]).

IV. CONCLUSION

This study proposed an approach for extracting low-dimensional time series of latent features from multi-dimensional driving behaviour data using DSAE where Hyperbolic Tangent is set as activation function, the cost function integrated a L2 penalization term and a Kullback-Leibler divergence term.

From a theoretical point of view, the low-dimensional time series of latent features extracted using DSAE proved useful for driving behaviour visualization. Feature extraction were robust against defects and outliers. This is a direct consequence of the training method used on the DSAE, namely the back-propagation method that minimize the square error between the input data and the reconstructed data. The research demonstrated also that dataset with high correlated inputs features obtained best results in term of defects reparability and latent features extraction.

The obtained driving color maps represent an immediate visualization tool considering the potential impacts on road safety of driver behaviour recognition from large datasets. It is possible to evaluate this first attempt as a successfully one, as resulting in marked capability of the method to recognize road complexity and a satisfying capacity to visualize external events (i.e. pedestrians walking on crosswalk).

For future studies is envisaged the necessity to involve different categories of experimental variables in order to go beyond the limit of using only one typology of data (kinematic data). In particular, it is expected that physiological drivers' measurements (i.e. oculometry, direct measure of workload) and road conditions, if implemented, would add significance to the graphical output.

ACKNOWLEDGMENT

The authors thank the students Simone Frisco and Giorgia Bulgarelli for their valuable effort.

REFERENCES

[1] *Global Status Report on Road*, World Health Organization, Geneva, Switzerland, 2018, p. 20.
[2] U. Kramer, "On the application of fuzzy sets to the analysis of the system driver-vehicle-environment," *Automatica*, vol. 21, no. 1, pp. 101–107, Jan. 1985.
[3] S. Wold, K. Esbensen, and P. Geladi, "Principal component analysis," *Chemometrics Intell. Lab. Syst.*, vol. 2, nos. 1–3, pp. 37–52, 1987.
[4] C. Zhao, C. Zheng, and M. Zhao, "Classifying driving mental fatigue based on multivariate autoregressive models and kernel learning algorithms," in *Proc. 3rd Int. Conf. Biomed. Eng. Informat.*, Oct. 2010, pp. 2330–2334.
[5] W. Dong, J. Li, R. Yao, C. Li, T. Yuan, and L. Wang, "Characterizing driving styles with deep learning," Cornell Univ., New York, NY, USA, Tech. Rep. 1607.03611, 2016.
[6] K. Dwivedi, K. Biswaranjan, and A. Sethi, "Drowsy driver detection using representation learning," in *Proc. IEEE Int. Advance Comput. Conf. (IACC)*, Feb. 2014, pp. 995–999.
[7] J. Meseguer, C. T. Calafate, J. C. Cano, and P. Manzoni, "Characterizing the driving style behavior using artificial intelligence techniques," in *Proc. 38th Annu. IEEE Conf. Local Comput. Netw. (LCN)*, 2013, pp. 4–6.
[8] H. Wu, H. Gao, S. Wang, and D. Jiang, "Recognition of road type for unmanned vehicle based on texture and color features," in *Proc. 2nd Int. Conf. Image, Vis. Comput. (ICIVC)*, Jun. 2017, pp. 189–193.
[9] Z. Camlica, A. Hilal, and D. Kulic, "Feature abstraction for driver behaviour detection with stacked sparse auto-encoders," in *Proc. IEEE Int. Conf. Syst., Man, (SMC)*, Oct. 2016, pp. 3299–3304.
[10] H. Liu, T. Taniguchi, Y. Tanaka, K. Takenaka, and T. Bando, "Visualization of driving behavior based on hidden feature extraction by using deep learning," *IEEE Trans. Intell. Transp. Syst.*, vol. 18, no. 9, pp. 2477–2489, Sep. 2017.
[11] P. Thomas, B. Price, C. Paine, and M. Richards, "Stacked denoising autoencoder," *J. Educ. Technol.*, vol. 33, no. 5, pp. 537–549, 2002.
[12] J. Zhang, Z. Wu, F. Li, C. Xie, T. Ren, J. Chen, and L. Liu, "A deep learning framework for driving behavior identification on in-vehicle can-bus sensor data," *Sensors*, vol. 19, no. 6, p. 1356, Mar. 2019.
[13] J. Guo, Y. Liu, L. Zhang, and Y. Wang, "Driving behaviour style study with a hybrid deep learning framework based on GPS data," *Sustainability*, vol. 10, no. 7, p. 2351, Jul. 2018.
[14] V. Vignali, F. Cuppi, E. Acerra, A. Bichicchi, C. Lantieri, A. Simone, and M. Costa, "Effects of median refuge island and flashing vertical sign on conspicuity and safety of unsignalized crosswalks," *Transp. Res. F, Traffic Psychol. Behav.*, vol. 60, pp. 427–439, Jan. 2019.
[15] M. Costa, A. Bichicchi, M. Nese, C. Lantieri, V. Vignali, and A. Simone, "T-junction priority scheme and road user's yielding behavior," *Transp. Res. F, Traffic Psychol. Behav.*, vol. 60, pp. 770–782, Jan. 2019.
[16] G. Di Flumeri, "EEG-based mental workload assessment during real driving: A taxonomic tool for neuroergonomics in highly automated environments.," *Neuroergonomics*, vol. 12, pp. 121–126, Jan. 2019.
[17] G. Di Flumeri, "EEG-based mental workload neurometric to evaluate the impact of different traffic and road conditions in real driving settings," *Front. Hum. Neurosci.*, vol. 12, pp. 1–18, Dec. 2018.
[18] S. G. Hart and L. E. Staveland, "Development of NASA-TLX," *Hum. Ment. Workload. Adv. Psychol.*, no. 52, pp. 139–183, Jan. 1988.

ARIANNA BICHICCHI received the master's degree in civil engineering from the University of Bologna, in 2011, with a specialization in infrastructures and transportation. She is currently pursuing the Ph.D. degree with the XXXI cycle at the DICAM Department, School of Engineering, University of Bologna, with a research project entitled innovative technologies for road—users interaction analysis, who proposes to analyze the contribution of the human factors in road safety. She has coauthored several scientific publications focusing on the use of Eye Tracker and electroencephalographic headset (EEG) for the evaluation of drivers' attention, inattention, and workload.

RACHID BELAROUSSI received the master's degree in physics from ESPCI, the master's degree in electronics from UPMC, and the Ph.D. degree in computer vision on appearance-based model (auto-encoder) applied to face detection, in 2006. He joined the French Institute of Science and Technology for Transport (IFSTTAR), in 2011. He has worked since on vehicle perception and driver characterization.

ANDREA SIMONE has been an Associate Professor with the School of Engineering and Architecture, University of Bologna, since 2004. He has served on European and international (AIPCR-PIARC) technical committees. He has authored about 100 publications. His main research areas are mobility analysis and design, highway design, road safety analysis, road safety design, and human factor interaction.

VALERIA VIGNALI received the Ph.D. degree in transportation engineering (civil engineering). She is currently an Assistant Professor with the Department of Civil, Chemical, Environmental, and Materials Engineering, School of Engineering and Architecture, University of Bologna. Her research interests concern road, railway and airport infrastructures, with particular reference to the analysis of the road-drivers interaction by innovative technologies. She authored numerous scientific articles published in international journals.

CLAUDIO LANTIERI received the Ph.D. degree in transportation engineering. He has been a Junior Assistant Professor, since 2016 and a Senior Assistant Professor, since 2019 with the School of Engineering and Architecture, University of Bologna. He has been teaching and Teaching Assistant in all courses of the DICAM—Roads area, with activities assistant supervisor in several dissertations. He has been a member of the SIIV (Italian Society of Road Infrastructures), since 2006, he has participated in several conferences and seminars and has authored publications in journals and national and international conferences on topics related to the subject area ICAR04.

XUANPENG LI received the Ph.D. degree from University Paris Sud, in 2014, on the study of vehicle safety based on multisource information fusion for ADAS. In 2015, he joined Southeast University as Assistant Professor. His is interested in evidence theory for driver inattention estimation and machine learning for 3D semantic mapping and visual signal language recognition.